Visco-acoustic full waveform tomography of synthetic ocean bottom seismic data

N. Damodara[1, 2,*], Kalachand Sain[1, 2]

[1]*CSIR -National Geophysical Research Institute (NGRI), Hyderabad 500 007, India.*
[2]*Academy of Scientific and Innovative Research (AcSIR), CSIR-NGRI Campus, Hyderabad 500 007, India.*
[*]e-mail: *naradamu@gmail.com*

Keywords: Ocean bottom seismometer; waveform tomography; frequency-domain; elastic and acoustic data.

Summary

Though lot of theoretical studies has been carried out, still we lack in understanding the state-of-the-art full waveform tomography (FWT) tool. To know the intricacies involved in FWT, we pursue a theoretical study for a realistic earth model derived from the well log data. We generate the wide-angle ocean bottom seismic (OBS) data based on visco-elastic finite difference modeling and perform the FWT in acoustic sense in deriving the best possible result. From different choices of multi-scale imaging in frequency domain, we observe that the frequency overlapping is more suitable in mitigating the highly non-linearity of the tomographic inversion.

Introduction

The state-of-the-art full waveform tomography (FWT) of seismic data can further improve the long-wavelength velocity model generated by the conventional travel time tomography by exploiting the entire components (times, amplitudes, frequencies...) of seismic wave field. Over the past few decades, it has been implemented by several pioneering researchers around the globe both in time-domain (Kolb et al., 1986; Gauthier et al., 1986; Mora, 1987) and in frequency-domain (Pratt and Worthington, 1990; Pratt, 1990a, b; Geller and Hara, 1993; Song et al., 1995) by using implicit numerical algorithms. For technical review, one can read the classic paper by Virieux and Operto (2009).

The FWT is very sensitive to many factors starting from the algorithm of the problem to initial model and many intermediate stages involved. Here we demonstrate the sensitivity of the frequency selection for the frequency-domain FWT from the synthetic seismic data generated for a realistic earth model. Due to page-limitation we present only a brief overview of the exercise.

Data

We have created a two-dimensional P-wave velocity model of 50.0 *km* long and 5.0 *km* depth (Fig.1) by correlating two available well log data. The S-wave velocity and the density models are derived from the Vp model using the following relations (1) & (2) respectively.

$$V_s(m/s) = 0.8619\ x\ V_p - 1172 \qquad (1)$$

$$\rho(g/cc) = 0.31\ x\ \left(V_p\right)^{0.25} \qquad (2)$$

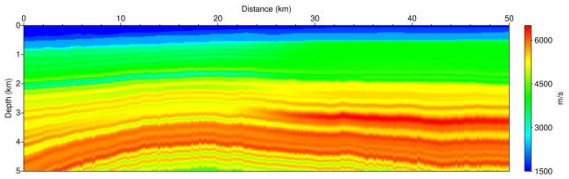

Fig.1. True model used for generating elastic data.

The OBS data have been generated based on finite-difference elastic modeling using the normalized Ricker wavelet with central frequency of 10 Hz (Bohlen, 1998, 2002). This includes computation of 51 OBS data with 1.0 km interval. The recording length is 16.384 s with sampling interval 4 *ms*.

Full waveform tomography

We apply the visco-acoustic full waveform tomography to the generated data in the frequency domain (Dessa et al, 2004; Operto et al., 2004, 2006; Ravaut et al., 2004). The smoothed version (Fig.2) of the true model has been taken as the initial model for FWT. Further, we select the frequency (i) as per the criteria defined by Sirgue & Pratt (2004) and (ii) continuous set of frequencies with constant interval.

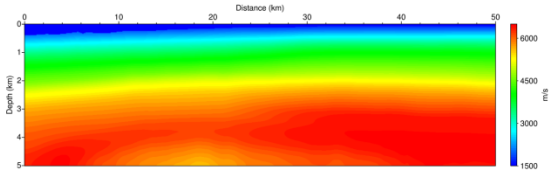

Fig.2. Smoothed version of true model.

With these, we formulate following four cases, and present the results.

Case 1: Smooth model-Continuous frequency set-without overlapping
Case 2: Smooth model-Continuous frequency set-with overlapping
Case 3: Smooth model-Optimal frequency set-without overlapping
Case 4: Smooth model-Optimal frequency set-with overlapping

In case 1, we use the continuous discrete set of total 40 frequencies starting from 2 Hz to 21.5 Hz with an interval 0.5 Hz. These 40 frequencies are formed into 20 groups (ex., group 1: 2, 2.5 Hz; group 2: 3.0, 3.5 Hz; group 3: 4.0, 4.5 Hz; etc.) with each group having 2 frequencies without overlapping between them.

In case 2, we use same frequencies as in case 1, but formed into 39 groups by overlapping the single frequency between the groups (ex., group 1: 2, 2.5 Hz; group 2: 2.5, 3.0 Hz; group 3: 3.0, 3.5 Hz; etc.). The FWT uses two frequencies at a time.

In case 3, we select the frequency as per the criteria of Sirgue & Pratt (2004) that will be contributed by two frequencies 2 Hz and 10.2 Hz between minimum 2 Hz and maximum of 20 Hz. To stabilize the inversion we further added 4 additional frequencies (1.95, 19.54, 20.03, 20.1 Hz) and inverted sequentially all 6 frequencies without overlapping between groups.

In case 4, we use the same strategy as used in case 3. Further we form all 6 frequencies into 4 frequency groups with each group having 3 frequencies by overlapping between them (ex., group 1: 1.95, 2.02, 10.2 Hz; group 2: 2.02, 10.2, 19.54 Hz; group 3: 10.2, 19.54, 20.03 Hz; group 4: 19.54, 20.03, 20.1 Hz).

Before applying the frequency-domain acoustic FWT, we follow necessary preprocessing steps like bandpass filtering, muting etc. so that the data satisfies the acoustic principle (Dessa et al, 2004; Operto et al., 2004, 2006; Ravaut et al., 2004). Fig.3 shows before and after preprocessing the data. All inversion parameters for each case are the same except specified above in each group. The final results of FWT for each case are shown in Fig.4.

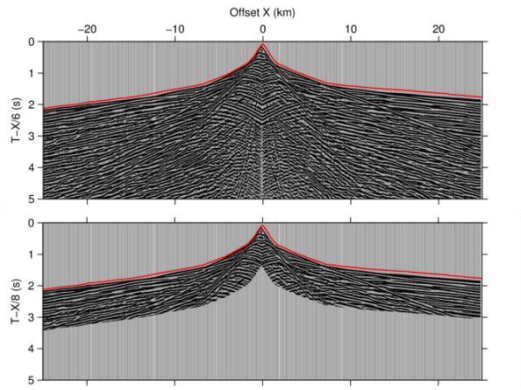

Fig.3. Elastic data generated from true model (top). Preprocessed data before applying FWT (bottom). The first arrival picks are marked with red color.

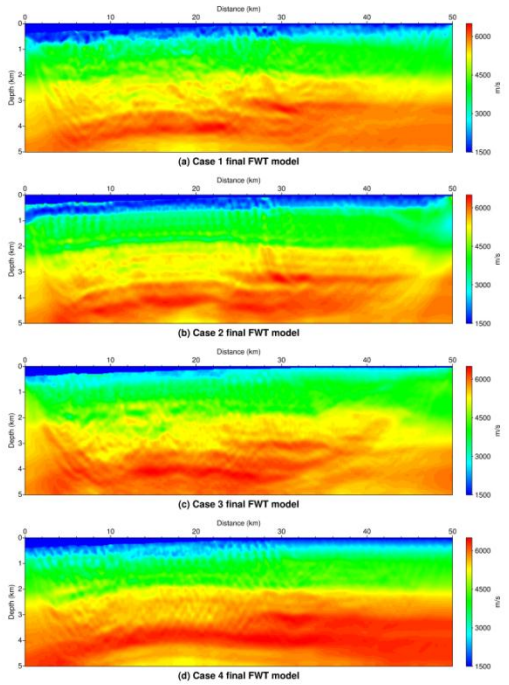

Fig.4. Final models obtained after full waveform tomography for Cases 1, 2, 3 and 4 from top to bottom respectively.

The constant density and attenuation models are used during the FWT rather than using known models. The 1-D velocity-depth functions derived at two different positions viz. 17.9 *km* and 28.9 *km* are compared with the true models in figure 5.

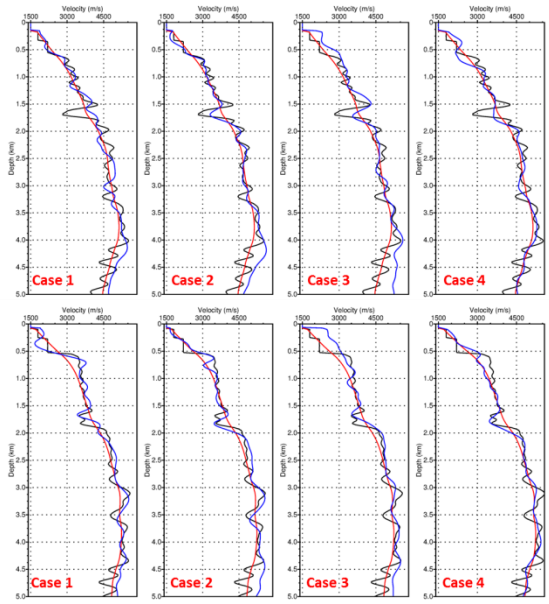

Fig.5. The extracted 1-D-models with true 1-D models at 17.9 *km* (top panel) and at 28.9 *km (bottom panel)* respectively Black curves -true models, Red curves - smooth models (initial model before FWT) and Blue curves - final FWT models for respective case.

Conclusions

It is obvious that the FWT can delineate finer details of the subsurface, which are not evident in the initial model. Since the FWT is very highly computational intensive, these types of synthetic case studies are very useful in understanding the practical issues and intricacies involved. The study shows that the multiscale imaging with overlapping in the frequency groups with continuous interval (case 2) always produce the best possible result (Figs 4 &5). Since, we have performed the full waveform tomography for the elastic wave data in acoustic sense using the constant density and attenuation, there lies a tremendous scope for pursuing research for successful application of FWT to real seismic data.

Acknowledgements

The Director, CSIR-NGRI is acknowledged for permission to present this work. The developers of different modeling & Inversion open source packages and, the Generic Mapping Tools (Wessel & Smith 1998) are acknowledged. The first author (ND) thanks CSIR for providing him with the CSIR-SRF fellowship. This is a contribution to scientific research of CSIR-NGRI under MLP-6402-28(KS).

References

Bohlen, T. 1998. Interpretation of Measured Seismograms by Means of Viscoelastic Finite Difference Modeling. Ph.D. thesis, Kiel University.

Bohlen, T. 2002. Parallel 3-D viscoelastic finite-difference seismic modeling. Comput. and Geosci., 28(8), 887–899.

Dessa, J. X., Operto, S., Kodaira, S., Nakanishi, A., Pascal, G., Virieux, J., & Kaneda, Y., 2004. Multiscale seismic imaging of the eastern Nankai trough by full waveform inversion. Geophys. Res. Letters, 31, L18606.

Gauthier, O., Virieux, J., and Tarantola, A. (1986). Two-dimensional nonlinear inversion of seismic waveforms: numerical results. Geophysics, 51(7):1387–1403.

Geller, R. J., and Hara, T. (1993). Efficient algorithms for iterative linearized inversion of seismic wave-form data: Geophysical Journal International, 115, 699–710.

Kolb, P., Collino, F., and Lailly, P. (1986). Prestack inversion of 1-D medium,. In Extended Abstracts, volume 74, 498–508.

Mora, P. R. (1987). Nonlinear two-dimensional elastic inversion of multi-offset seismic data Geophysics, 52:1211–1228.

Operto, S., Ravaut, C., Improta, L., Virieux, J., Herrero, A., & Dell'Aversana, P., 2004. Quantitative imaging of complex structures from dense wide-aperture seismic data by multiscale traveltime and waveform inversions: a case study. Geophysical Prospecting, 52: 625-651.

Operto, S., Virieux, J., Dessa, J. X., & Pascal, G., 2006. Crustal seismic imaging from multifold ocean bottom seismometer data by frequency-domain full-waveform tomography: application to the eastern-Nankai trough. Journal of Geophysical Research, 111(B09306).

Pratt, R. G. (1990a). Frequency-domain elastic modeling by finite differences: a tool for crosshole seismic imaging. Geophysics, 55(5): 626-632.

Pratt, R. G. (1990b). Inverse theory applied to multi-source cross-hole tomography. Part II: elastic wave-equation method. Geophysical Prospecting, 38:311–330.

Pratt, R. G. and Worthington, M. H. (1990). Inverse theory applied to multi-source cross-hole tomography. Part 1: acoustic wave-equation method. Geophysical prospecting, 38:287-310.

Ravaut, C., Operto, S., Improta, L., Virieux, J., Herrero, A., & Dell'Aversana, P., 2004. Multiscale imaging of complex structures from

multifold wide-aperture seismic data by frequency-domain full-waveform tomography: application to a thrust belt. Geophys. J. Int., 159: 1032-1056.

Sain, K., and Damodara, N., Sensitivity analysis of different factors during frequency domain visco-acoustic full waveform tomography. working paper.

Sirgue, L. and Pratt, R. G. (2004). Efficient waveform inversion and imaging: a strategy for selecting temporal frequencies. Geophysics, 69(1):231–248.

Song, Z. M., Williamson, P. R., and Pratt, R. G. (1995). Frequency-domain acoustic-wave modeling and inversion of crosshole data, Part 2: Inversion method, synthetic experiments and real-data results: Geophysics, 60, 796–809.

Virieux, J., Operto, S., 2009. An overview of full waveform inversion in exploration geophysics. Geophysics, 74, WCC1-WCC26.

Wessel, P. and Smith, W.H.P., 1998. New improved version of generic mapping tools released, EOS, Trans. Am. geophys. Un., 79(47), 579.